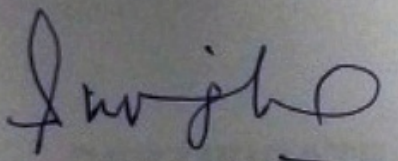

CERTIFICATE

It is certified that the work contained in the thesis titled "*Effect of Semi-solid Processing on Microstructure and Tribological Characteristics of Al-10Cu alloy*" by "*Sankara Rao L.*" has been carried out under our supervision and this work has not been submitted elsewhere for a degree.

It is further certified that the student has fulfilled all the requirements of Comprehensive, Candidacy and SOTA.



Prof. S. N. Ojha

(Supervisor)



Prof. A. K. Jha

(Co-Supervisor)

Department of Metallurgical Engineering
Indian Institute of Technology
(Banaras Hindu University)

Department of Mechanical Engineering
Indian Institute of Technology
(Banaras Hindu University)

DECLARATION BY THE CANDIDATE

I, "*Sankara Rao L.*", certify that the work embodied in this thesis is my own bona fide work and carried out by me under the supervision of "*Prof. S. N. Ojha and Prof. A. K. Jha*" from "*July 2012*" to "*Jan 2018*", at the "*Department of Metallurgical Engineering*", Indian Institute of Technology (BHU), Varanasi. The matter embodied in this thesis has not been submitted for the award of any other degree/diploma. I declare that I have faithfully acknowledged and given credits to the research workers wherever their works have been cited in my work in this thesis. I further declare that I have not willfully copied any other's work, paragraphs, text, data, results, *etc.*, reported in journals, books, magazines, reports dissertations, theses, *etc.*, or available at websites and have not included them in this thesis and have not cited as my own work.

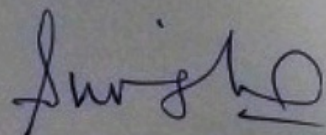
Date

Place


Sankara Rao L.

CERTIFICATE BY THE SUPERVISORS

It is certified that the above statement made by the student is correct to the best of our knowledge.


Prof. S.N. Ojha
(Supervisor)

Department of Metallurgical Engineering
Indian Institute of Technology
(Banaras Hindu University)


Prof. A.K. Jha
(Co-Supervisor)

Department of Mechanical Engineering
Indian Institute of Technology
(Banaras Hindu University)


Head

Department of Metallurgical Engineering
Indian Institute of Technology
(Banaras Hindu University)

विभागाध्यक्ष/HEAD

धातुकीय अभियांत्रिकी विभाग
Deptt. of Metallurgical Engg.

भारतीय प्रौद्योगिकी संस्थान (काशी हिन्दू विश्वविद्यालय)
Indian Institute of Technology (Banaras Hindu University)
वाराणसी-221005/Varanasi-221005

COPYRIGHT TRANSFER CERTIFICATE

Title of the Thesis: *"Effect of Semi-solid Processing on Microstructure and Tribological Characteristics of Al-10Cu alloy"*

Name of the Student: *Sankara Rao L.*

COPYRIGHT TRANSFER

The undersigned hereby assigns to the Indian Institute of Technology (Banaras Hindu University) Varanasi all rights under copyright that may exist in and for the above thesis submitted for the award of the *"Ph.D. Degree"*.

Date:

Place:

L. Sankara Rao
Sankara Rao L.

Note: However, the author may reproduce or authorize others to reproduce material extracted verbatim from the thesis or derivative of the thesis for author's personal use provided that the source and the Institute's copyright notice are indicated.

ACKNOWLEDGEMENTS

I am indebted to Prof. S. N Ojha, Department of Metallurgical Engineering, my supervisor, for his constant encouragement, support and guidance during the entire period of my research work. The way he teaches me is really excellent and he is always source of inspiration for me. He always supported me in both research and in personal problems. He is always my best teacher. I would not have been able to complete the thesis without his utmost involvement and invaluable efforts.

I sincerely thank my co-supervisor Prof. A. K. Jha, for his invaluable guidance for the thesis work. He has also rendered constant encouragement and support during the course of this thesis work.

I sincerely thank Prof. N. K. Mukhopadhyay, Head of the Department of Metallurgical Engineering for providing all the research facilities to successfully accomplish my research in the Department Besides my Supervisors, I would like to thank other members of RPEC: Prof. Santhosh Kumar, Department of Mechanical Engineering, Dr. J. K. Singh, Department of Metallurgical Engineering and also Dr. C. K. Behera (DPGC Member), for their insightful comments and encouragement. I have deep sense of gratitude to Prof. R. K. Mandal, Prof. Sunil Mohan, Dr N. K. Prasad, Prof. I. Chakrabarty, and all other faculty members of the Department of Metallurgical Engineering, IIT (BHU), for their cooperation and inspiration.

I am obliged to all my seniors, friends and juniors specially Mr Santosh Kumar Alla, Dr. Gaurav Gautam, Dr. Narendra Kumar, and Dr. Arup Kumar Mandal, Mr. M. Dhanunjay for their constant encouragement, making joyful and memorable life being with my moments of

happiness and troubles at IIT (BHU), Varanasi. I am also thankful to all my junior students of M. Tech and PhD of our group from 2012 to 2016 for their constant support during fatigue testing. I am thankful to all the Lab and Main workshop staff specially Mr Raj Narayan, Kamalesh, Rajendar, and Chotelalji for making wear and tensile specimens, Shri Ashok Kumar Ji for helping in scanning electron microscopy, and all the office staff. I am thankful to wonderful seniors and friends Dr. S. K. Mandal and B. Rajak for their constant encouragement, making joyful and memorable life being with my moments of happiness and troubles at IIT (BHU), Varanasi.

Last, but not the least, I would like to express my deepest gratitude to my family for their unconditional support and encouragement to pursue my interest.

I also wish to thank all my friends and the persons whose names have not been mentioned on this piece of paper for extending their cooperation directly or indirectly.

Sankara Rao L.

*Dedicated to
My Family
and
Supervisors*

CONTENTS

	Page No.
List of Figures	vii
List of Tables	xiii
Preface	xv
Chapter 1: An Overview of Semi-Solid Processing	
	1-23
1.1 Introduction.....	
	1
1.2 Semi-solid Processing Techniques.....	
	2
1.2.1 Rheocasting.....	
	3
1.2.2 The cooling slope Process (CSP).....	
	7
1.2.3 Semi -Solid Rheocasting (SSR TM Casting).....	
	9
1.2.4 Strain Induced Melt Activation (SIMA) Process	
	10
1.2.5 Spray casting (Osprey process).....	
	12
1.2.6 Thixocasting process.....	
	14
1.2.7 Thixomoulding.....	
	15
1.3 Microstructures of Semi-solid Processed Alloys.....	
	15
1.3.1 Dendrite Fragmentation Mechanism.....	
	15
1.3.2 Micro/Macro Structure Analysis.....	
	16
1.4 Wear Characteristics of Semi-Solid processed Alloys.....	
	19

1.4.1 Adhesive Wear.....	19
1.4.2 Abrasive Wear.....	20
1.4.3 Corrosive Wear.....	22
1.4.4 Surface Fatigue wear	23
1.4.5 Cavitation.....	23
Chapter 2: Solidification of Liquid Distributed in its Matrix	25-51
2.1 Introduction.....	25
2.2 Experimental Details.....	26
2.2.1 Preparation of Al-10Cu alloy.....	26
2.2.2 Thermal cycling of as cast alloy.....	27
2.2.3 Microstructural examination.....	28
2.2.4 Wear testing.....	28
2.3 Results and discussion.....	29
2.3.1 Undercooling behaviour.....	29
2.3.2 Microstructural features.....	30
2.3.3 Wear characteristics of alloy.....	37
2.4 Conclusions.....	51
Chapter 3: Rheocasting of Al-10Cu Alloy and its tribological characteristics and surface topography	53-87
3.1 Introduction.....	53

3.2 Experimental Details.....	55
3.2.1 Preparation of alloy and wear samples.....	55
3.2.2 Rheocasting Procedure.....	55
3.2.3 Metallography and Mechanical Testing.....	56
3.2.4 Wear testing.....	56
3.3 Results and discussion.....	57
3.3.1 Microstructural Features.....	57
3.3.2 Mechanical Testing.....	64
3.3.3 Wear Characteristics	66
3.3.3.1 Effect of Process Variables	66
3.3.3.2 Load and sliding velocity	69
3.3.3.3 Morphology of worn-out surfaces.....	72
3.4 Conclusions.....	87
Chapter 4: Microstructure and Tribological Characteristics of SIMA	89-132
Processed Alloy	
4.1 Introduction.....	89
4.2 Experimental Details.....	92
4.2.1 Preparation of metal mould casting	92
4.2.2 Solidification temperature range.....	93
4.2.3 Preparation of Stirred Metal Mould Casting	94
4.2.4 SIMA processing technique	94

4.2.5 Metallography procedures.....	95
4.2.6 Mechanical Testing	96
4.2.7 Wear testing procedures	97
4.3 Results and Discussion.....	98
4.3.1 Microstructural Features.....	98
4.3.2 Mechanical properties.....	113
4.3.3 Wear characteristics of alloy.....	116
4.3.4 Morphology of wornout surfaces.....	121
4.4 Conclusions.....	132

Chapter 5: Tribological Characteristics of Centrifugal Cast Alloy 135-174

5.1 Introduction.....	135
5.2 Experimental details.....	137
5.2.1 Centrifugal casting process variables.....	137
5.2.2 Metallography.....	138
5.2.3 Mechanical Testing.....	139
5.2.4 Wear study.....	139
5.3 Results and Discussion.....	140
5.3.1 Microstructural features	141
5.3.2 Mechanical properties.....	158
5.3.3 Wear characteristics.....	164
5.4 Conclusions.....	174

Overall Conclusions..... 175
Scope of the Future Work..... 176
References..... 177

List of Figures

Figure 1.1	Two different mechanisms for rheocasting process.	2
Figure 1.2	Semi-Solid processing by Rheocasting.	4
Figure 1.3	Direct Slurry Formation (DSF) process and machine components.	5
Figure 1.4	Schematic of electromagnetic coils for MHD stirring and solid particle flow pattern in the mushy zone (a) due to rotational inductive coils, (b) due to linear inductive coils, and (c) helicoidal stirring reproduced from [Niedermaier et al. 1998].	6
Figure 1.5	Schematic of the new rheo-casting process (NRC) NRC: pouring – controlled cooling – sleeve filling – forming.	7
Figure 1.6	Schematic of the Cooling slope process.	8
Figure 1.7	Schematic of the SSR process. Molten alloy is held above the liquidus (Step 1), then rapidly cooled and agitated for a controlled duration to a temperature below the liquidus (Step 2) before agitation and cooling ceases (Step 3).	9
Figure 1.8	Schematic illustration of the stages of the SIMA process.	10
Figure 1.9	Process stages of the RAP method.	11
Figure 1.10	Schematic illustration of the experimental setup of spray forming.	13
Figure 1.11	Schematic diagram of Thixocasting process.	14
Figure 1.12	Formation of cramped dendrite: (a) bright field illumination, (b) polarized light, A356 alloy quenched at 598 °C.	17
Figure 1.13	Definition of pseudo-particles and pseudo-clusters, (b) CAD generated view of a 3D rendered pseudo-cluster.	18
Figure 1.14	X-ray microtomography of Al–15.8%Cu held at 555°C for 80 min, (a) globules with various sizes, visible dissolution of globule 1 over time, (b) globule with equal size, coalescence toward formation of a single particle.	19

Figure 1.15	Steps leading to Adhesive Wear.	20
Figure 1.16	Abrasion in the microscale.	21
Figure 1.17	Schematic of abrasive Wear Phenomena.	22
Figure 1.18	Schematic of fatigue wear, due to the formation of surface and subsurface cracks.	23
Figure 2.1	Schematic diagram showing thermal cycles of the alloy from 560 °C from different hold time (a) single cycle for 5hrs (b) four cycles for 5hr holding time.	27
Figure 2.2	Typical inverse rate cooling curve of Al-10Cu alloy.	30
Figure 2.3	Optical micrographs of (a) as cast alloy showing dendritic structure and (b) to (d) cast alloy subjected to four thermal cycle from 560 to 300 °C held for 5hrs showing a progressive change in size and size distribution of liquid phase.	33
Figure 2.4	SEM micrographs of four thermal cycled alloy at 560 °C hold for 5hrs (a) liquid pockets distributed in the matrix (b) liquid droplets entrained in the grains thermal cycle.	35
Figure 2.5	(a) EDS analysis of the droplets formed during the 4 th thermal cycle of the Al-10Cu alloy, (b) EDS analysis of the solid matrix on which droplets were formed during the 4 th thermal cycle.	37
Figure 2.6	Variation of cumulative volume loss with sliding distance (a) at 10N (b) at 20N (c) at 30N (d) at 40N (e) at 50N.	40
Figure 2.7	Variation of wear rate as a function of normal load of the as cast and thermal cycled alloys.	41
Figure 2.8	Variation of coefficient of friction with (a) sliding distance (b) normal load.	43
Figure 2.9	SEM micrographs of worn surfaces of the as cast alloy at two different loads (a) 30N (b) 50N showing increasing dimple structure with increase in applied load.	45

Figure 2.10	SEM micrographs of worn surfaces of a as cast after the first thermal cycle at different loads (a) 30N (b) 50N.	48
Figure 2.11	SEM micrographs of worn surfaces of a as cast after the fourth thermal cycle at different loads (a) 30N (b) 50N.	49
Figure 2.12	SEM micrographs and corresponding EDS of the wear track at 1m/s sliding velocity and load of 50N.	50
Figure 3.1	Optical micrographs of Al-10Cu alloy produced by (a) metal mould casting and (b) rheocasting at 400 rpm stirring speed.	58
Figure 3.2	Optical micrographs and grain size distribution of Al-10Cu alloy produced by rheocasting method at (a) 800 rpm, (b) 1200 rpm stirring speed.	60
Figure 3.3	SEM micrograph of Al-10Cu alloy produced by rheocasting method at a stirred speed of (a) 800 rpm, (b) 1200 rpm.	62
Figure 3.4	EDS analysis results of rheocast alloy at (a) 800 rpm, (b) 1200 rpm.	64
Figure 3.5	Effect of stirring speed on the (a) hardness and (b) ultimate tensile strength of Al-10Cu alloy produced by metal mould casting (MMC) and rheocasting (RC).	65
Figure 3.6	The variation in cumulative volume of the samples produced by metal mould casting and rheocasting at different stirred speeds with (a) sliding distance (b) load and (c) sliding velocity.	68
Figure 3.7	The variation in wear rate of metal mould cast and rheocast alloys with (a) load and (b) sliding velocity.	70
Figure 3.8	The variation in coefficient of friction of metal mould cast and rheocast alloys with (a) load and (b) sliding velocity.	72
Figure 3.9	SEM micrographs of worn surfaces at 30N load and 1m/s sliding velocity for (a) Metal mould cast alloy (b) 400 rpm (c) 800 rpm and (d) 1200 rpm of rheocast alloys.	74
Figure 3.10	SEM micrographs and EDS analysis of 1200 rpm stirring speed rheocast sample worn surfaces tested at 30 N load and 5 m/s sliding velocity at (a) lower and (b) higher magnifications.	76
Figure 3.11	SEM micrographs and EDS analysis of 800 rpm stirring speed	78

	rheocast sample worn surfaces tested at 30 N load and 5 m/s sliding velocity at (a) lower and (b) higher magnifications.	
Figure 3.12	SEM micrographs and EDS analysis of 400 rpm stirring speed rheocast sample worn surfaces tested at 30 N load and 5 m/s sliding at (a) lower and (b) higher magnifications.	79
Figure 3.13	Line analysis and 3D profilometer image for rheocast with 800 rpm stirring speed at 50 N load and 1 m/s sliding velocity.	81
Figure 3.14	Line analysis and 3D profilometer image for rheocast with 1200 rpm stirring speed at 50 N load and 1 m/s sliding velocity.	82
Figure 3.15	Line analysis and 3D profilometer image for the alloy produced by rheocasting with 800 rpm stirring speed at 30 N load and 3 m/s sliding velocity.	83
Figure 3.16	Line analysis and 3D profilometer image for rheocast alloy with 1200 rpm stirring speed at 30 N load and 3 m/s sliding velocity.	84
Figure 3.17	Line analysis and 3D profilometer image for the alloy produced by rheocasting with 800 rpm stirring speed at 30 N load and 5 m/s sliding velocity.	85
Figure 3.18	Line analysis and 3D profilometer image for the alloy produced by rheocasting with 1200 rpm stirring speed at 30 N load and 5 m/s sliding velocity.	86
Figure 4.1	Al-Cu phase diagram.	93
Figure 4.2	DSC measurement of Al-10Cu Alloy.	94
Figure 4.3	Metal Mould (a) schematic diagram, (b) picture, (c) casting sample.	96
Figure 4.4	Tensile testing sample (a) schematic diagram, (b) picture.	97
Figure 4.5	Wear testing sample (a) schematic diagram, (b) picture.	98
Figure 4.6	Optical Micrographs of Al-10Cu alloy (a) Metal Mould Casting, (b)-(f) SIMA processed sample at 580 °C. The holding times for (b) to (f) are 10, 30, 40, 45, and 55 minutes respectively.	103
Figure 4.7	Grain size distribution of SIMA processed samples of Al-10Cu alloy at 580 °C with holding times (a) 10 minutes, (b) 30 minutes, (c) 40	106

minutes, (d) 45 minutes and (e) 55 minutes. These correspond to the microstructures in Fig. 2(b)-(f).

Figure 4.8	Optical microscopy and grain distribution of SIMA processed Al-10Cu alloy sample at 580 °C with holding time 30 minutes of stirred MMC.	107
Figure 4.9	EDS analysis results of stirred MMC upon 50% pre-deformation followed by heating at 580 °C for 30 minutes (a) matrix, (b) eutectic globular droplet and (c) grain boundary.	110
Figure 4.10	Results from line analysis in SIMA processed stirred MMC at eutectic grain boundary.	111
Figure 4.11	Results from line analysis in SIMA processed stirred MMC at primary phase matrix.	112
Figure 4.12	Graphs of Al-10Cu alloy (a) ultimate tensile strength vs. processing method, (b) hardness vs. processing method.	114
Figure 4.13	The SEM microstructures of a fractured surface of tensile specimens (a) MMC (b) MMC subjected to SIMA and (c) stirred MMC subjected to SIMA.	116
Figure 4.14	Variation of cumulative volume loss with sliding distance MMC, MMC subjected to SIMA and stirred MMC subjected to SIMA at (a) 10N, (b) 20 N, (c) 30 N, and (d) 40 N.	120
Figure 4.15	(a) variation of wear rate as a function of normal load, (b) variation of the coefficient of friction with sliding distance at 40 N of MMC, MMC subjected to SIMA and stirred MMC subjected to SIMA.	121
Figure 4.16	Worn surface topography of the Metal mould casting (MMC) at 40 N load and 1 m/s sliding velocity under SEM and profilometer.	124
Figure 4.17	Worn surface topography of the Metal mould casting (MMC) at 40 N load and 1 m/s sliding velocity under SEM and profilometer.	126
Figure 4.18	Worn surface topography of the MMC subjected to SIMA at 40 N load and 1 m/s sliding velocity under SEM and profilometer.	129
Figure 4.19	Worn surface topography of the stirred MMC subjected to the SIMA	132

process at 40 N load and 1 m/s sliding is sliding velocity under SEM and profilometer.

- | | | |
|--------------------|---|-----|
| Figure 5.1 | Microstructure of Al-10Cu casting at a speed of 800 rpm (a) outer (b) central (c) inner regions and histograms of grain size distribution of primary α -phase. | 145 |
| Figure 5.2 | Microstructure of Al-10Cu casting at a speed of 1320 rpm (a) outer (b) central (c) inner regions and histograms of grain size distribution of primary α -phase. | 148 |
| Figure 5.3 | Microstructure of Al-10Cu casting at a speed of 1980 rpm (a) outer (b) central (c) inner regions and histograms of grain size distribution of primary α -phase. | 151 |
| Figure 5.4 | Microstructure of Al-10Cu casting at a speed of 2850 rpm (a) outer (b) central (c) inner regions and histograms of grain size distribution of primary α -phase. | 154 |
| Figure 5.5 | Microstructure of stir cast Al-10Cu casting at a speed of 1980 rpm (a) outer (b) central (c) inner regions and histograms of grain size distribution of primary α -phase. | 157 |
| Figure 5.6 | Graphs of (a) Hardness versus mould speed and (b) Ultimate tensile strength versus mould speed of centrifugal castings. | 160 |
| Figure 5.7 | SEM microstructures of fractured surface of tensile specimens (a) Metal mould casting and Centrifugal castings at (b) 800 rpm (c) 1320 rpm (d) 1980 rpm (e) 2850 rpm (f) 1980 rpm with stirring. | 163 |
| Figure 5.8 | Variation of cumulative volume loss with sliding distance at (a) 10 N (b) 20 N (c) 30 N (d) 40 N (e) 50 N. | 167 |
| Figure 5.9 | (a) Variation of wear rate as a function of normal load of metal mould casting and (b) Variation of coefficient of friction with sliding distance. | 169 |
| Figure 5.10 | SEM micrographs of worn surfaces of Al-10Cu alloys at a load of 50N (a) Metal mould casting and Centrifugal casting at (b) 800 rpm (c) 1320 rpm (d) 1980 rpm (e) 2850 rpm (f) 1980 rpm with stirring. | 173 |

145 **List of tables**

148 **Table 2.1** Chemical composition of Al-10Cu alloy. 27

Table 3.1 Chemical Composition of Al-10Cu Alloy. 55

151 **Table 5.1** Chemical composition of Al-10Cu alloy as measured by Emission
arc spectrometer. 138

154

157

160

63

67

69

73

PREFACE

Aluminium alloys find a wide range of applications in automotive and aerospace industries due to their high specific strength and ability to be cast into complex shape. However, a cast product is known to have coarse dendritic structure and macro segregation. Consequently, there is continuous endeavor to the development of new processing techniques for in-process modification of the microstructure. The semi-solid processing techniques fulfil this criterion and research efforts in this direction have led to development of a large number of processing techniques. In these techniques, the alloys are held in semi-solid region at different temperature and time. These are also subjected to the stirring to create a slurry and cast into a die for making desired shape of the component after solidification of the melt. Even though there are many variants of semi-solid processing techniques, a proper understanding of liquid distribution in the matrix phase and its solidification behaviour have not been systematically studied. These understanding will facilitate processing of even unconventional alloy with their effective control of the microstructure and better tribological behaviour. The present investigation has been carried out with this objective. A wide freezing range Al-10Cu alloy has been selected for processing employing different semi-solid processing techniques and critical evaluation of their tribological characteristics.

This thesis consists of five chapters. **Chapter-1** presents an overview of semi-solid processing techniques and their characteristics features. The microstructural features of the alloy and techniques employed for their characterization have been discussed. The morphological

features of the primary phase and eutectics and mechanisms of their formation have been brought out.

Chapter 2 comprises the investigation of solidification of liquid phase entrained in its primary solid. A hypo-eutectic alloy based on Al-Cu-Fe system containing Fe and Si was thermal cycled between semi-solid region to low temperatures. The freezing characteristics of the liquid were recorded in inverse rate cooling curves. The continuous network of the liquid phase progressively changed into isolated droplets with their different size and size distribution. Such droplets revealed undercooling of the melt varying from 20 to 35°C below the eutectic temperature of the alloy. This behaviour of melt undercooling is discussed in light of independent nucleation events associated with freezing of droplets. Solidification structure of droplets revealed particulate eutectic phases in contrast to lamellar eutectic microstructure in the inter-dendritic region of the as cast alloy. The decomposition of supersaturated solid solution phase resulting from large undercooling of droplets were explained for this anomalous behavior of the eutectic. The hardness of the matrix as well as that of droplet solidified areas were examined and found 152 HV for the matrix and 267 HV for its droplets. The wear property of the alloy was studied in a range of load varying from 10-50 N at sliding velocity 1.0 m/s. The droplet distribution and their solidification structure resulted in an improvement in tribological characteristics of the alloy. This effect is attributed to the presence of ultrafine solidification structure of droplets arising from their large undercooling. This feature is evident in the microstructure of droplet regions. In addition, the solute elements are themselves get redistributed differently in droplets vis-a-vis that in the liquid present in the inter-dendritic region of the cast alloy. The EDAX analysis of droplet regions and that of the bulk liquid region provides support in this direction. This effect is correlated with features of wear surfaces generated on the matting surfaces.

Chapter-3 includes the investigation of Al-10Cu alloy containing small amount of Fe and Si which were produced by rheocasting process at different mechanical stirring speeds. The resultant microstructures and wear properties were compared with that of a conventional metal mould cast alloy. The average grain size was measured to be 55 μm for the 800 rpm and 30 μm for the alloy melt stirred at 1200 rpm samples respectively. The rheocast alloys have shown better mechanical (ultimate tensile strength and hardness) and wear properties as compared to metal mould cast alloy. Moreover rheocast alloy which was produced at 1200 rpm stirring speed exhibited enhanced wear and mechanical properties as compared to other rheocast alloys. The improved wear rate for this alloy was attributed to finer grain size and the nearly-spherical morphology of the primary α - phase. The metal mould cast alloy and rheocast alloy at 400 rpm have shown adhesive wear condition whereas, other rheocast alloys have displayed microcutting mechanism of wear. The noticeable decrease in the average roughness for 3 m/s sliding velocity was observed as compared to a sliding velocity of 1 m/s. In addition, the average roughness value of the 1200 rpm stirred alloy is observed to be lower than that of the alloy produced at 800 rpm stirring speed.

Chapter-4 deals with the study of influence of synthesis methods, namely, the conventional metal mould casting (MMC) followed by strain induced melt activation (SIMA) processes, on the microstructure and tribological characteristics of Al-10Cu alloy. The alloy was prepared by melting the commercial purity aluminium and copper. The effect of holding time in semi-solid region on the microstructure of the alloy subjected to SIMA was studied. Microstructural characterization was performed using optical and scanning electron microscopy, while chemical segregation is investigated using energy dispersive spectroscopy. Hardness and

strength of the resulting alloy are measured using macroindentation and tensile testing, respectively. Near-spherical grains were achieved in the SIMA process with an average grain diameter varying from 45 to 65 μm for holding times ranging from 30 to 55 minutes. The wear properties of stirred MMC alloy which was subjected to SIMA process are considerably better than those of either conventional MMCs or unstirred MMC subjected to SIMA process. The 50% pre-deformation followed by intercritical annealing at 580 °C and 30 minutes holding time are the optimum parameters for to obtain such a wear properties of Al-10Cu alloy. The improved wear and mechanical properties of the alloy are discussed in light of the microstructural features of SIMA processed alloy and the nature of the worn surfaces.

Chapter-5 presents the study of producing Al-10Cu alloy by vertical centrifugal casting at speeds ranging from 800-2850 rpm. The microstructural features, mechanical and wear properties have been investigated. The wall thickness of stirred centrifugal cast Al-10Cu alloy is uniform from top to bottom resulting in a sound casting. The variation in thickness of casting from top to bottom is 25 mm for 800 rpm, 7 mm for 1320 rpm, 1 mm for 1980 and 10 mm for 2850 rpm. The microstructure of Al-10Cu alloy consists of equiaxed grain morphology of the primary α -phase with eutectic phases in the interdendritic regions. It has been observed that there is a variation in the grain size from the inner surface of the casting to its outer surface. The speed also has a strong influence on the grain size and subsequent mechanical properties of the alloy. The tensile strength and hardness of stirred centrifugal cast alloy were observed to be 181 MPa and 150 HV which are higher than that of the other alloys. The wear properties of the alloy have been evaluated at a constant sliding velocity of 1 m/s for a range of applied load and sliding distance. The optimum mould speed was found to be 1980 rpm as it produced fine microstructure in the casting resulting in optimum hardness, ultimate tensile strength and wear rate. The cumulative volume loss and

consequent wear rate of stirred centrifugal cast alloy are invariably lower than that of the other alloys under study. The worn surface of stirred centrifugal cast alloy appears to be less damaged than that of the other centrifugal alloys. This is because of the reason that the driving force acting on the molten metal at optimum speed was sufficient enough to carry the molten metal to the inner surface of the mould and hold firmly there before it get solidified resulting in a uniform cylindrical casting. The variations in the wear behavior are attributed to the size and solidification morphology of the castings.

The conclusions of the present thesis work are summarised and have been presented in the section that follows. It is noteworthy to observe that amongst various semi-solid processes investigated in the present work, the SIMA process resulted in considerable refinement of the primary phase with change in its morphology to round shape. The constituent of the eutectic phases in the inter-dendritic region exhibited globular shape. The understanding of morphological changes have been explained on the nature of distribution of liquid explained on the nature of distribution of liquid either along grain inter-dendritic region or within the solid phase as isolated droplets. The detail study of the solidification behaviour of such liquids exhibit several interesting features and considerable change in tribological characteristics of the alloys. These features are discussed in detail.